Suplemento de la Revista Mexicana de Física 3 040921 (2022) 1–7

Influence of heavy resonances in SMASH

J. Salinas San Martín and J. Noronha-Hostler
Illinois Center for Advanced Studies of the Universe,
Department of Physics, University of Illinois at Urbana-Champaign, 1110 W. Green St., Urbana IL 61801-3080, USA

H. Elfner
GSI Helmholtzzentrum für Schwerionenforschung, Planckstr. 1, 64291 Darmstadt, Germany
Institute for Theoretical Physics, Goethe University, Max-von-Laue-Strasse 1, 60438 Frankfurt am Main, Germany
Frankfurt Institute for Advanced Studies, Ruth-Moufang-Strasse 1, 60438 Frankfurt am Main, Germany
Helmholtz Research Academy Hesse for FAIR (HFHF), GSI Helmholtz Center,
Campus Frankfurt, Max-von-Laue-Strasse 12, 60438 Frankfurt am Main, Germany

J. Hammelmann
Institute for Theoretical Physics, Goethe University, Max-von-Laue-Strasse 1, 60438 Frankfurt am Main, Germany
Frankfurt Institute for Advanced Studies, Ruth-Moufang-Strasse 1, 60438 Frankfurt am Main, Germany

R. Hirayama
Institute for Theoretical Physics, Goethe University, Max-von-Laue-Strasse 1, 60438 Frankfurt am Main, Germany
Frankfurt Institute for Advanced Studies, Ruth-Moufang-Strasse 1, 60438 Frankfurt am Main, Germany
Helmholtz Research Academy Hesse for FAIR (HFHF), GSI Helmholtz Center,
Campus Frankfurt, Max-von-Laue-Strasse 12, 60438 Frankfurt am Main, Germany

Received 3 July 2022; accepted 15 September 2022

Recent lattice QCD results, comparing to a hadron resonance gas model, have shown the need for hundreds of particles in hadronic models. These extra particles influence both the equation of state and hadronic interactions within hadron transport models. Here, we introduce the PDG21+ particle list, which contains the most up-to-date database of particles and their properties. We then convert all particles decays into 2 body decays so that they are compatible with SMASH in order to produce a more consistent description of a heavy-ion collision.

Keywords: ***Heavy-ion collision, Resonances, Equation of State, SMASH***

1 Introduction

In the 1960's Rolf Hagedorn envisioned the particle spectrum to be composed of fireballs consistent of fireballs. The idea was that very heavy hadronic resonances decayed into somewhat less heavy resonances, which would in turn decay to even lighter resonances. He showed this effect in his seminal paper [1] using resonances up to the $\Delta(1232)$ baryon that the hadronic resonances followed an exponential mass spectrum, demonstrated by experiments over the course of the last two decades as more and more particles have been identified [2–5].

To study the strong interaction further, heavy-ion collision experiments collide atomic nuclei at relativistic speeds and track their collective flow through charged particles. Heavy-ion collisions offer a unique opportunity to study an out-of-equilibrium many-body system, which crosses the QCD phase transition from deconfined quarks and gluons into hadrons. To accurately model a heavy-ion collision, several different stages involving different physical phenomena have to be used: initial condition, pre-equilibrium, hydrodynamics, hadronization, and hadronic afterburner. Through out the modeling of heavy-ion collisions, it is important that the equation of state is consistent with the rest the modeling. At the point of hadronization one must switch from quarks and gluons as the degrees of freedom into hadrons. Those hadrons and their interactions must be consistent with the hadronic part of the equation of state. This implies that if one creates a state-of-the-art equation of state but uses a hadronic afterburner with a mismatch in particles, it can cause a number of problems. Thus, theorists are careful to always match the hadrons in the equation of state (EOS) to that of the hadronic afterburner (see [6–8]).

Simulating Many Accelerated Strongly-interacting Hadrons (SMASH) is a state-of-the-art hadron transport code that is widely used as afterburner after hydrodynamic simulations and standalone for relatively low-energy heavy-ion collision simulations [9, 10]. The approach followed by SMASH is based on the relativistic Boltzmann equation, where the collision term in the low-energy regime is dominated by binary hadron scatterings and excitation and decay of resonances, i.e., by $2 \leftrightarrow 2$ and $1 \leftrightarrow 2$ reactions, respectively, where the degrees of freedom are the well-established hadronic resonances and their corresponding properties [9, 11]. Recently, SMASH has been used to investigate the effects of a high-density medium on fluctuation

observables, hadronic potentials, jet quenching, and baryon, photon and deuteron production among others, leading to similar results to those of other implementations of microscopic transport models [9, 11–22].

It has been shown that the inclusion of more hadronic resonances when creating EOSs leads to significant changes in transport coefficients [23–26] and observables like the elliptic flow coefficient v_2 [27], susceptibilities [28], p_T spectra [7, 29], and chemical freeze-out conditions [30], especially in the strange sector. For example, in Refs. [28, 31] the μ_S/μ_B ratio was calculated to leading order in μ_B, as function of susceptibilities of conserved charges, within the Hadron Resonance Gas (HRG) model using different resonance lists, showing a better agreement with lattice data up to the transition temperature when more hadronic states are considered. Moreover, the authors of [28] also demonstrate that other related observables, such as χ_4^S/χ_2^S and χ_{11}^{us}, indicate that that the inclusion of addition of $|S| = 1$ baryons and mesons is favorable, as opposed to multi-strange resonances.

Current equations of state use the PDG16+ particle list [28], an exhaustive compendium of resonances and their properties taken from the Particle Data Book [32]. With the motivation of using a transport code that includes the same resonances as the EOS used for hydrodynamic stages, we have revised the PDG16+ to create the PDG21+ list, which has the updated masses and decays of all known experimentally measured particles. In total, 24 new particles were added –mostly in the strange baryon sector– and 10 were taken out, modifying the Hagedorn spectrum, as well as updating previous- and adding several new decay channels. Massive resonances in particular have been shown (experimentally) to decay into three or four particle decays. On the other hand, due to the geometrical collision criterion used in SMASH, only $1 \to 2$ decays are normally considered, with the exception of recent efforts to implement a stochastic treatment [17, 33]. The PDG21+ list was then adapted to be used in SMASH using intermediate states to account for multi-body decays.

2 PDG21+ resonance list

Over the past 5 years experiments have shed light on new particle resonances, providing better information on their masses and known decay channels compared to what was known in 2016 when the PDG16+ was created. Here we build on the previous PDG16+ list that includes the particles and properties, including particle ID (PID), mass, width, degeneracy, baryon number, strangeness content, isospin, electric charge, and branching ratios of decay channels. The PDG16+ contemplated 408 different particles, of which 153 were mesons and 255 are baryons.

An extensive revision of the PDG16+ was carried out, updating the values of mass and width, as well as decay channels and branching rations to the most recent experimental data available. For heavier resonances (mass $\gtrsim 1.5$ GeV), it becomes more and more common to have missing decay channels, i.e., the reported branching ratios do not add up to 1. In the 16+ edition of the list, a ratio of 90%–10% was assigned for unknown and known decay channels, respectively, where unknown decay channels were modeled as radiative decays to a relatively lighter hadron. In the case of the 21+ edition, the experimentally reported ratio was kept as is, only using radiative decays as a complement to obtain the 100% of decays. Recent experimental results, such as the observations in [34–36], provided new knowledge of the branching ratios of heavy resonances, especially in the Σ and Λ sectors, thus relaxing the need of approximations.

In the Review of Particle Physics, particles are organized according to a confidence level scale, depending on the amount of evidence to back up the existence of each particle and their properties. The most well-established states are marked with four stars (****), whilst resonances that have minimal information are given one star (*). As was shown in [28], 1-2 star states are fundamental to describe lattice results. To qualify as an entry for the PDG21+, it was generally sufficient for the candidate resonance to have one star of confidence level and to be located under the Particle Listings section of the Particle Data Book [5]. Notice that some particles in the Review are labeled as *Further States* and are not included in the PDG21+ due to the overall lack of information for such states. Moreover, some states in the Listings section have also been omitted; such is the case of $\Lambda(2585)$ or $\Sigma(3000)$. Only light and strange hadrons are considered for particle and decay channel listings, leaving charm and bottom hadrons out, as well as leptons. The new version of the list contains 418 different particles, of which 151 are mesons and 267 are baryons.

Particle name	Status
$a_1(1420)$	deleted
$X(1840)$	deleted
$\pi_2(2005)$	added
$X(2370)$	added
$a_6(2450)$	deleted
$\Sigma(1770)$	deleted
$\Sigma(1840)$	deleted
$\Sigma(2000)$	deleted
$\Sigma(2010)$	added
$\Sigma(2160)$	added
$\Sigma(2230)$	added
$\Sigma(2455)$	added
$\Sigma(2620)$	added
$\Sigma(3170)$	added
$\Lambda(2070)$	added
$\Lambda(2080)$	added
$\Omega(2012)$	added

TABLE I. Newly added and deleted particles in the PDG21+ list. It is understood that each particle includes all the elements of the corresponding multiplet and their antiparticles.

Particle name
$\Sigma(1730) \to \Sigma(1780)$
$\Sigma_+(1940) \to \Sigma(1940)$
$\Sigma_-(1940) \to \Sigma(1910)$
$\Lambda(2020) \to \Lambda(2085)$

TABLE II. Renamed particles in the PDG21+ list. It is understood that each particle includes all the elements of the corresponding multiplet and their antiparticles.

A total of 24 particles were added and 10 were removed with respect to the PDG16+ list. In Table I, a complete list of the particles added and removed are shown. In addition, some particles were renamed, and are shown in Table II; these are states that kept the same quantum numbers but had their mass updated under newly available experimental information. In Fig. 1 we present a comparison of the particle spectra per hadronic species between the previous PDG16+ and the new PDG21+ lists, including the more restrictive PDG21 version, which only includes states with a 3-star degree of certainty or more; it is clear that more resonances have been included and of particular interest, particles with strange content, which are precisely the ones where lattice results suggested new resonances could better explain the data.

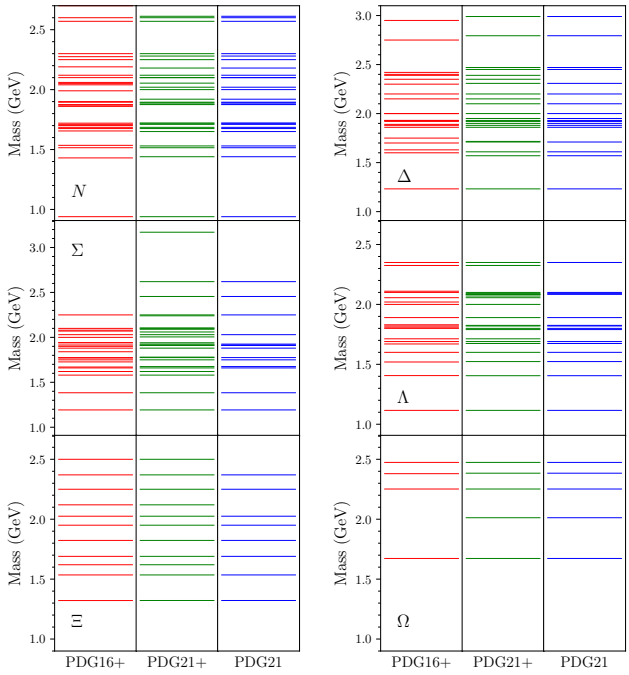

FIGURE 1. Particle spectra per species as extracted from the PDG16+ and PDG21+ lists. The newer list contains more resonances and updated properties for previously known particles.

Hadron resonance gas models are commonly used to study the thermodynamics of the hadronic phase of QCD matter, which can be extracted from the a partition function whose only free parameters are the number of particle resonances and their masses. Early on, it was predicted by Hagedorn that the number of hadronic resonances with respect of mass would grow exponentially, that is,

$$\rho(m) = f(m)\exp(m/T_H), \tag{1}$$

where $f(m)$ is a slowly varying function of m and T_H is a free-parameter known as the Hagedorn limiting temperature, understood soon after as the temperature at which the hadronic description breaks down [2–4].

Despite its simplicity, the HRG model is in good agreement with lattice data up to temperatures close to the phase transition temperature [27] and presents itself as a tool to create new EOSs. Hence, it becomes necessary to study the behavior of the particle spectrum as new particles are considered, since these changes will have an effect on the corresponding Hagedorn temperature. In Fig. 2 we show the particle spectra for all particles in the PDG21+ list, compared to those included on the default SMASH release, along with the corresponding fits to data, using a version of Eq. 1 given by

$$\rho(m) = \int_{m_0}^{m} \frac{A}{[M^2 + M_0^2]^{5/4}}\, e^{M/T_H}\, dM \tag{2}$$

Although the extracted limiting temperature is highly sensitive to the mass cutoff, it is found that the Hagedorn temperature is lower in the case of the new list, $T_H^{\text{PDG21+}} \simeq 170$ MeV, than the one coming from the particle set in SMASH, $T_H^{\text{SMASH}} \simeq 179$ MeV, approaching the phase transition temperature of ~ 155 MeV.

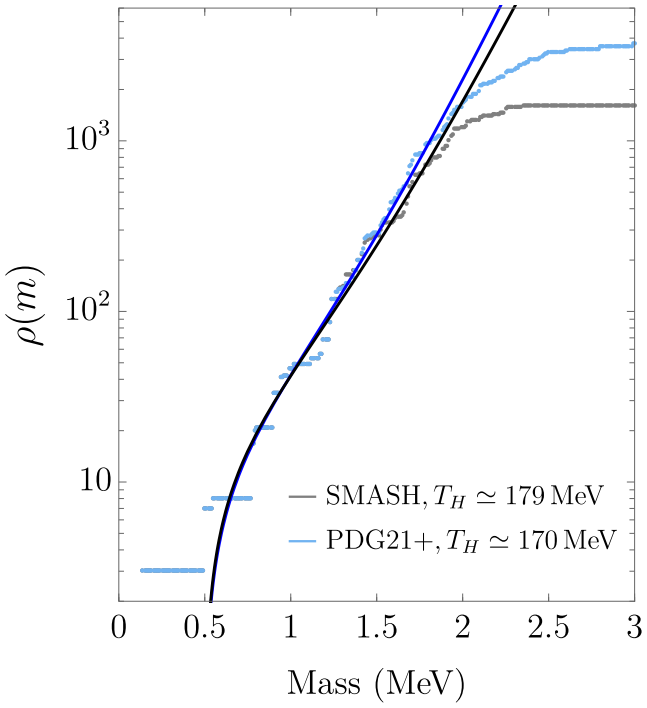

FIGURE 2. Particle spectra for the well-established states included in SMASH (gray) and the full PDG21+ list (light blue) with the corresponding fits of Eq. 2 shown in black and blue, respectively, and the respective Hagedorn temperatures.

3 Implementation in SMASH

The Quark Gluon Plasma is described by relativistic viscous hydrodynamics that rapidly expands and cools in time until particles cool enough to become hadrons. After hadronization, the particles are still interacting with other hadrons, which can be described through hadron transport models. These models are crucial to make direct comparisons to experimental data because experiments can only measure the final state particles.

Here we use the hadron transport code, SMASH [9, 10] that is an open-source code written in C++ that is commonly used in the field following the hydrodynamic phase [18, 20, 37–40]. The current version of SMASH has 222 states and their decay channels. Because both PDG16+ and PDG21+ have significantly more states, it is not possible to run an EOS, such as [41,42], that is based upon the PDG16+ list in a hydrodynamic model and then use SMASH in its current format.

The reason for the mismatch between the most current PDG lists and SMASH is because it is not straightforward to simply add new, heavy resonances into SMASH. The main barrier is that SMASH cannot handle $1 \to 3$ or $1 \to 4$ body decays. There are computational difficulties in handling the back reactions, i.e., $3 \to 1$ and $4 \to 1$ and without those back reactions detailed balanced would no longer be preserved. However, eliminating particles with these channels also isn't the solution since many heavy resonances decay into 3+ particles. Thus, the solution has been to convert $1 \to 3$ or $1 \to 4$ into decays with an intermediate resonance that then provides the same final state. For example, the $f_0(1500)$ hadron has 12 decay channels and one of them goes to $\pi^+\pi^+\pi^-\pi^-$. We can then include an intermediate decay $f_0(1500) \to \rho^0\rho^0$, since each ρ^0 meson will then also decay into two pions, i.e., $\rho^0 \to \pi^+\pi^-$. In this manner the final state has been preserved, although the decay itself is slightly slowed down by passing through an intermediate channel.

The correct identification of an intermediate state required a number of steps. For each heavy resonance with a 3 or 4-body decay, the least massive 2-particle intermediate state that could further decay into the final state was chosen. Furthermore, the lowest possible absolute value for the angular momentum L was also chosen for each decay channel, depending on the daughter particles, since SMASH enforces angular momentum conservation in decays. In the few cases where was no possible intermediate state, or it violated mass conservation, the mass of the parent particle was increased as long as the increment was small compared to the original mass. Nonetheless, wherever this was not viable, such decay channels were deleted, having all other branching ratios normalized; this was the case for 25 decay channels. In cases where many possible intermediate states could in principle decay to the final state, only the one with the lowest combined mass was chosen, as it is the most energetically favored state.

One challenge with this method is that intermediate states may have other possible decay channels besides the preferred one. For example, the hyperon resonance $\Lambda(1690)$ decays into $\Sigma + \pi + \pi$ about 20% of the time, whose intermediate state is $\Sigma(1385) + \pi$, using $\Sigma(1385)$ as a proxy for the $\Sigma + \pi$ pair. However, the $\Lambda + \pi$ decay channel for the $\Sigma(1385)$ resonance is more usual than $\Sigma + \pi$.

To handle the connection between the PDG, standard formats used in the heavy-ion community, and SMASH, we have written a code that converts the output of our original table of particles (taken diretctly from the PDG) into the correct format, making all the adjustments discussed here. This code can output formats compatible with ThermalFIST [43] such that the PDG21+ can be used in thermal models as well. This new code also allows one to easily add new particles from further upgrades to the PDG such that we do not anticipate that one should have to wait every 5 years to upgrades the particle lists used within the heavy-ion community.

Once the new particles are in the SMASH format, they can then be implemented directly into SMASH. The first thing to test is the effect of these new states on the cross-sections.

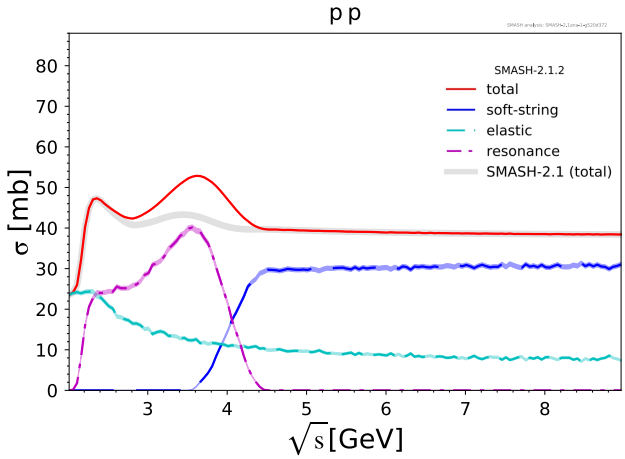

FIGURE 3. Proton-proton cross-section by type of process. The inclusion of new resonances and decay channels contribute to a bump in the total cross-section calculated using the PDG21+ decay list (red line) compared to the default SMASH list (gray line).

The cross-sections have already been measured experimentally and, therefore, they must reproduce experimental data. In Figs. 3 and 4, we present two examples, the pp and np, cross-sections. The red line is the total cross-section that has to match experimental data, the cyan line is the contribution of elastic processes, magenta stands for the contribution of resonances, blue is the contribution of string processes handled with the help of Pythia [44], and the gray line is the total cross-section without any of the 3 and 4-body decays included in SMASH, which matches experimental data. The contributions coming from resonances have increased significantly. There is a distinct bump in each of the plots, which occurs because of the inclusion of these new particles and

their corresponding decay channels. Now that the effect of including more resonances in SMASH has been shown, it is necessary to reproduce the experimental data for the elementary total cross-sections, which requires adjustments on their treatment within SMASH.

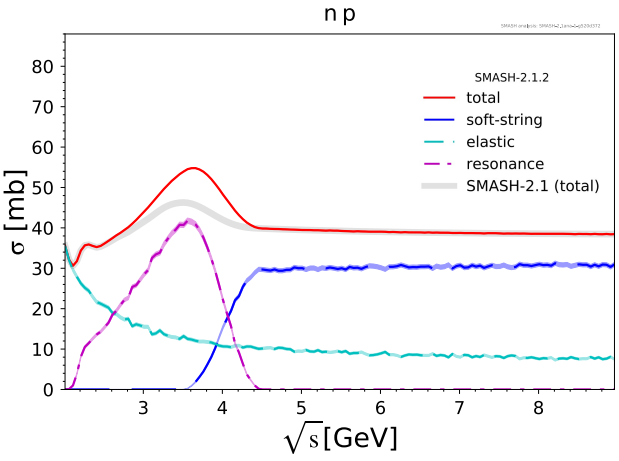

FIGURE 4. Neutron-proton cross-section by type of process. The inclusion of new resonances and decay channels contribute to a bump in the total cross-section calculated using the PDG21+ decay list (red line) compared to the default SMASH list (gray line).

4 Conclusions

Experimental developments have lead to the discovery of new heavy hadronic resonances and better knowledge of their interactions over the past 5 years. In this work we have updated the particle list to the PDG21+ that includes formats that are compatible with both SMASH and ThermalFIST. As more particles are taken into consideration when building a new EOS, observables such as susceptibilities are modified, in many cases approaching a better description of lattice data. However, to be fully consistent, one has to be careful and use the same particle list and decays –as the one coming from the EOS– when using afterburners. In particular, we have compiled a new particle list, the PDG21+, with the latest Particle Data Book information available and adapted it to work with SMASH. The latter was done by modeling 3 and 4-body decays as a sequence of 2-body decays with intermediate states. To quantify the effect of new heavy resonances, we computed the total pp and np cross-sections, observing a bump coming from the newly added channels and hadronic states. In order to adapt the list in SMASH consistently with experimental data for elementary total cross-sections, more work is needed adjusting the internal framework; this is currently underway and the results will be published elsewhere. We will then explore the consequences of the addition of these new resonances both with SMASH comparisons to experimental data at low beam energies as well as hydrodynamics coupled to SMASH using a hybrid approach at high energies.

5 Acknowledgments

This work was supported in part by the NSF within the framework of the MUSES collaboration, under grant number OAC-2103680. J.N.H. acknowledges the support from the US-DOE Nuclear Science Grant No. DE-SC0020633. The authors also acknowledge support from the Illinois Campus Cluster, a computing resource that is operated by the Illinois Campus Cluster Program (ICCP) in conjunction with the National Center for Supercomputing Applications (NCSA), and which is supported by funds from the University of Illinois at Urbana-Champaign. J.H. acknowledges the support by the DFG SinoGerman project (project number 410922684).

1. R. Hagedorn, *Statistical thermodynamics of strong interactions at high energies*, Nuovo Cimento Suppl. **3** (1965) 147
2. W. Broniowski and W. Florkowski, *Different Hagedorn temperatures for mesons and baryons from experimental mass spectra, compound hadrons, and combinatorial saturation*, Phys. Lett. B **490** (2000) 223, https://doi.org/10.1016/S0370-2693(00)00992-8
3. J. Noronha-Hostler, *Implications of Missing Resonances in Heavy Ions Collisions*, In Excited Hyperons in QCD Thermodynamics at Freeze-Out (2016) pp. 118–127.
4. P. Man Lo, et al., *Missing baryonic resonances in the Hagedorn spectrum*, Eur. Phys. J. A **52** (2016) 235, https://doi.org/10.1140/epja/i2016-16235-6
5. P. Zyla et al., *Review of Particle Physics*, Prog. Theor. Exp. Phys. **2020** (2020) 083C01, https://doi.org/10.1093/ptep/ptaa104
6. J. S. Moreland and R. A. Soltz, *Hydrodynamic simulations of relativistic heavy-ion collisions with different lattice quantum chromodynamics calculations of the equation of state*, Phys. Rev. C **93** (2016) 044913, https://doi.org/10.1103/PhysRevC.93.044913
7. P. Alba, et al., *Effect of the QCD equation of state and strange hadronic resonances on multiparticle correlations in heavy ion collisions*, Phys. Rev. C **98** (2018) 034909, https://doi.org/10.1103/PhysRevC.98.034909
8. J. M. Karthein, et al., *Strangeness-neutral equation of state for QCD with a critical point*, Eur. Phys. J. Plus **136** (2021) 621, https://doi.org/10.1140/epjp/s13360-021-01615-5
9. J. Weil, et al., *Particle production and equilibrium properties within a new hadron transport approach for heavy-ion collisions*, Phys. Rev. C **94** (2016) 054905, https://doi.org/10.1103/PhysRevC.94.054905
10. D. Oliinychenko, et al., smash-transport/smash: SMASH-

2.1 (2021), https://doi.org/10.5281/zenodo.5796168.

11. J. Staudenmaier, N. Kübler, and H. Elfner, Particle production in AgAg collisions at $E_{\rm Kin} = 1.58A$ GeV within a hadronic transport approach, Phys. Rev. C **103** (2021) 044904, https://doi.org/10.1103/PhysRevC.103.044904

12. J. Mohs, S. Ryu, and H. Elfner, Particle Production via Strings and Baryon Stopping within a Hadronic Transport Approach, J. Phys. G **47** (2020) 065101, https://doi.org/10.1088/1361-6471/ab7bd1

13. A. Schäfer, et al., A Non-Equilibrium Approach to Photon Emission from the Late Stages of Relativistic Heavy-Ion Collisions, Nucl. Phys. A **1005** (2021) 121772, https://doi.org/10.1016/j.nuclphysa.2020.121772

14. D. Oliinychenko, C. Shen, and V. Koch, Deuteron production in AuAu collisions at $\sqrt{s_{NN}}$ =7–200 GeV via pion catalysis, Phys. Rev. C **103** (2021) 034913, https://doi.org/10.1103/PhysRevC.103.034913

15. H. Elfner, et al., *Jet quenching in the hadron gas: an exploratory study*, PoS **HardProbes2020** (2021) 155, https://doi.org/10.22323/1.387.0155

16. A. Sorensen and V. Koch, *Phase transitions and critical behavior in hadronic transport with a relativistic density functional equation of state*, Phys. Rev. C **104** (2021) 034904, https://doi.org/10.1103/PhysRevC.104.034904

17. J. Staudenmaier, et al., *Deuteron production in relativistic heavy ion collisions via stochastic multiparticle reactions*, Phys. Rev. C **104** (2021) 034908, https://doi.org/10.1103/PhysRevC.104.034908

18. A. Schäfer, et al., *Out-of-equilibrium photon production in the late stages of relativistic heavy-ion collisions*, Phys. Rev. C **105** (2022) 044910, https://doi.org/10.1103/PhysRevC.105.044910

19. T. Reichert, et al., *Comparison of heavy ion transport simulations: Ag + Ag collisions at E_{lab} = 1.58A GeV*, J. Phys. G **49** (2022) 055108, https://doi.org/10.1088/1361-6471/ac5dfe

20. A. Schäfer, et al., Particle production in a hybrid approach for a beam energy scan of Au+Au/Pb+Pb collisions between $\sqrt{s_{\rm NN}}$ = 4.3 GeV and $\sqrt{s_{\rm NN}}$ = 200.0 GeV (2021) arXiv:2112.08724

21. J. Hammelmann and H. Elfner, Impact of hadronic interactions and conservation laws on cumulants of conserved charges in a dynamical model (2022) arXiv:2202.11417

22. R. Hirayama, J. Staudenmaier, and H. Elfner, Effective spectral function of vector mesons via lifetime analysis (2022) arXiv:2206.15166

23. J. Noronha-Hostler, J. Noronha, and C. Greiner, *Transport Coefficients of Hadronic Matter near T(c)*, Phys. Rev. Lett. **103** (2009) 172302, https://doi.org/10.1103/PhysRevLett.103.172302

24. J. Noronha-Hostler, J. Noronha, and C. Greiner, *Hadron Mass Spectrum and the Shear Viscosity to Entropy Density Ratio of Hot Hadronic Matter*, Phys. Rev. C **86** (2012) 024913, https://doi.org/10.1103/PhysRevC.86.024913

25. J. Rais, K. Gallmeister, and C. Greiner, *Shear viscosity to entropy density ratio of Hagedorn states*, Phys. Rev. D **102** (2020) 036009, https://doi.org/10.1103/PhysRevD.102.036009

26. E. McLaughlin, et al., *Building a testable shear viscosity across the QCD phase diagram*, Phys. Rev. C **105** (2022) 024903, https://doi.org/10.1103/PhysRevC.105.024903

27. J. Noronha-Hostler, et al., *Elliptic Flow Suppression due to Hadron Mass Spectrum*, Phys. Rev. C **89** (2014) 054904, https://doi.org/10.1103/PhysRevC.89.054904

28. P. Alba, et al., *Constraining the hadronic spectrum through QCD thermodynamics on the lattice*, Phys. Rev. D **96** (2017) 034517, https://doi.org/10.1103/PhysRevD.96.034517

29. D. Devetak, et al., *Global fluid fits to identified particle transverse momentum spectra from heavy-ion collisions at the Large Hadron Collider*, JHEP **06** (2020) 044, https://doi.org/10.1007/JHEP06(2020)044

30. P. Alba, et al., *Influence of hadronic resonances on the chemical freeze-out in heavy-ion collisions*, Phys. Rev. C **101** (2020) 054905, https://doi.org/10.1103/PhysRevC.101.054905

31. A. Bazavov, et al., *Additional Strange Hadrons from QCD Thermodynamics and Strangeness Freezeout in Heavy Ion Collisions*, Phys. Rev. Lett. **113** (2014) 072001, https://doi.org/10.1103/PhysRevLett.113.072001

32. C. Patrignani et al., *Review of Particle Physics*, Chin. Phys. C **40** (2016) 100001, https://doi.org/10.1088/1674-1137/40/10/100001

33. O. Garcia-Montero, et al., *Role of proton-antiproton regeneration in the late stages of heavy-ion collisions*, Phys. Rev. C **105** (2022) 064906, https://doi.org/10.1103/PhysRevC.105.064906

34. A. V. Sarantsev, et al., *Hyperon II: Properties of excited hyperons*, Eur. Phys. J. A **55** (2019) 180, https://doi.org/10.1140/epja/i2019-12880-5

35. B. C. Hunt and D. M. Manley, *Updated determination of N^* resonance parameters using a unitary, multichannel formalis*m, Phys. Rev. C **99** (2019) 055205, https://doi.org/10.1103/PhysRevC.99.055205

36. F. Afzal, et al., *Observation of the $p\eta^{'}$ Cusp in the New Precise Beam Asymmetry Σ Data for $\gamma p \to p\eta$*, Phys. Rev. Lett. **125** (2020) 152002, https://doi/10.1103/PhysRevLett.125.152002

37. S. Ryu, J. Staudenmaier, and H. Elfner, *Bulk Observables within a Hybrid Approach for Heavy Ion Collisions with SMASH Afterburner*, MDPI Proc. **10** (2019) 44, https://doi.org/10.3390/proceedings2019010044

38. D. Oliinychenko, et al., *Microscopic study of deuteron production in PbPb collisions at $\sqrt{s} = 2.76TeV$ via hydrodynamics and a hadronic afterburner*, Phys. Rev. C **99** (2019) 044907, https://doi.org/10.1103/PhysRevC.99.044907

39. D. Everett et al., *Multisystem Bayesian constraints on the transport coefficients of QCD matter*, Phys. Rev. C **103** (2021) 054904, https://doi.org/10.1103/PhysRevC.103.054904

40. X.-Y. Wu, et al., *(3+1)-D viscous hydrodynamics at finite net baryon density: Identified particle spectra, anisotropic flows, and flow fluctuations across energies relevant to the beam-energy scan at RHIC*, Phys. Rev. C **105** (2022) 034909, https://doi.org/10.1103/PhysRevC.105.034909

41. P. Parotto, et al., *QCD equation of state matched to lattice data and exhibiting a critical point singularity*, Phys. Rev. C **101** (2020) 034901, https://doi.org/10.1103/PhysRevC.101.034901

42. J. Noronha-Hostler, et al., *Lattice-based equation of state at finite baryon number, electric charge and strangeness chemical potentials*, Phys. Rev. C **100** (2019) 064910, https://doi.org/10.1103/PhysRevC.100.064910

43. V. Vovchenko and H. Stoecker, *Thermal-FIST: A package for heavy-ion collisions and hadronic equation of state*, Comput. Phys. Commun. **244** (2019) 295, https://doi.org/10.1016/j.cpc.2019.06.024

44. T. Sjöstrand, S. Mrenna, and P. Skands, *A brief introduction to PYTHIA 8.1*, Comput. Phys. Commun. **178** (2008) 852, https://doi.org/10.1016/j.cpc.2008.01.036